35th EPS Conference on Plasma Phys. Hersonissos, 9 - 13 June 2008 ECA Vol.**32D**, P-2.043 (2008)

# Pseudochaotic poloidal transport in toroidal geometry: pressure-gradient-driven turbulence and plasma flow topology

I. Calvo[1], L. García[2], B. A. Carreras[3], R. Sánchez[4], and B. Ph. van Milligen[1]

[1] *Laboratorio Nacional de Fusión, Asociación EURATOM-CIEMAT, 28040 Madrid, Spain*

[2] *Universidad Carlos III, 28911 Leganés, Madrid, Spain*

[3] *BACV Solutions Inc., Oak Ridge, Tennessee 37830, USA*

[4] *Fusion Energy Division, Oak Ridge National Laboratory, Oak Ridge, Tennessee 37831, USA*

## Introduction

Three-dimensional numerical calculations of resistive pressure-gradient-driven turbulence in toroidal geometry show the existence of an unstable regime below the threshold for fully developed turbulence [1]. The transition from a stable plasma to this ballooning-mode-dominated regime has the characteristic properties of a topological instability [2]. We will study this unstable regime by means of a reduced set of MHD equations [3, 4], which in the electrostatic limit allow to write the flow velocity field in terms of a stream function: the electrostatic potential.

After the transition, the iso-surfaces of electrostatic potential induced by the ballooning modes have a complicated topological structure (see Figs. 1 and 2).

The structure of the potential iso-surfaces can be visualized as we move in the toroidal direction around the torus, following the magnetic field lines. At the singular magnetic surfaces, (potential) vortices emerge with a structure which is consistent with the local twist of the magnetic field lines. As the outermost part of torus (the low-field side) is approached, filamentary vortices from different singular surfaces may merge and form extended radial streamers. Radial transport takes place predominantly within these streamers, since particles can freely travel along them in the radial direction. The nature of radial transport within these streamers characterizes the confinement properties of the system. As we continue to follow the lines toroidally, the vortices move back into the high-field side and the streamers break up.

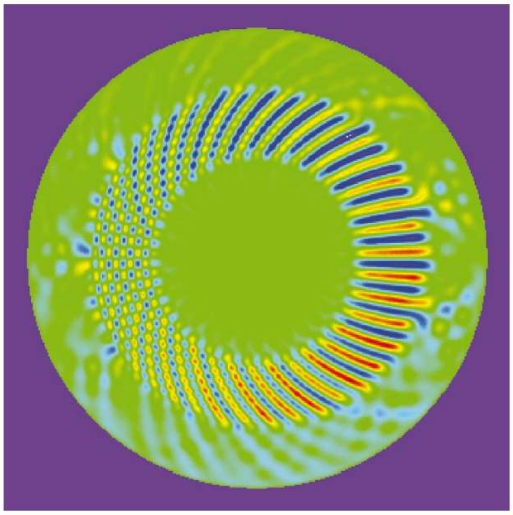

Figure 1: Contour plot of the velocity stream function in a toroidal cut

The present paper summarizes the results of [5], where we focus on poloidal transport. It

turns out to be an interesting example of $\alpha = 1$ anomalous diffusion.

The origin of this value of $\alpha$ is that, away from the streamers, particles simply spread out ballistically along the filaments while on the high-field side. Once they reach the low-field side again and enter a new streamer structure, their direction of motion can be modified as the new streamer breaks up to form a new set of filaments towards the high-field side and particles get trapped in them. It is this combination of ballistic motion plus scattering of velocity directions which is ultimately responsible of a Cauchy type (i.e., $\alpha = 1$) diffusive process.

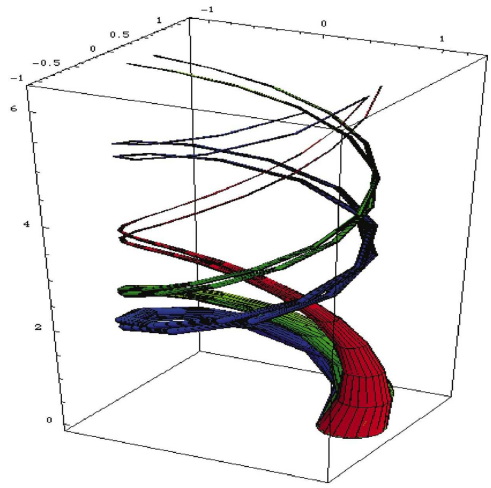

Figure 2: Representation of the filamentation of a streamer

**CTRWs on the circle**

Continuous Time Random Walks (CTRWs) are models describing the microscopic transport of particles in a probabilistic way. We are interested in the interpretation of poloidal transport in fusion plasmas as a CTRW defined on a circle. A general treatment of CTRWs on the circle has recently appeared [6].

A separable, Markovian, homogeneous time-translational invariant CTRW is defined by a mean waiting time, $\tau$, and a step-size pdf, $p(\Delta)$, giving the probability that a particle performs a jump from $x$ to $x+\Delta$. We denote by $n(\theta,t)$ the density of particles (tracer particles for the application of the formalism relevant to us) normalized to the total number of particles, i.e. $\int_0^{2\pi} n(\theta,t)\mathrm{d}\theta = 1,\ \forall t$. The function $n(\theta,t)$ must be periodic in $\theta$, $n(\theta+2\pi,t) = n(\theta,t)$. One would expect that the effect of the non-trivial topology of the circle be relevant and the CTRW on the circle should exhibit significant differences with respect to a CTRW with the same step-size pdf formulated on the real line.

As explained heuristically above, the relevant case for our purposes corresponds to $p(\Delta)$ being a Lévy distribution with index $\alpha = 1$, whose characteristic function (Fourier transform) is:

$$\hat{p}(k) = \exp(-\sigma|k| + i\mu k), \quad \sigma > 0,\ \mu \in \mathbb{R}. \tag{1}$$

We can give [6] a closed expression for the propagator of the fractional equation obtained as the hydrodynamic limit of this CTRW:

$$n(\theta,t) = \frac{1}{2\pi}\,\frac{\sinh(\sigma t/\tau)}{\cosh(\sigma t/\tau) - \cos(\mu t/\tau - \theta)}. \tag{2}$$

**Numerical calculations of tracer particle transport**

Now, we can compare the analytical predictions with the numerical data. We refer to [1, 5] for the details on the reduced MHD equations and the numerical scheme used to solve them.

The first results of particle tracer transport have been obtained by launching 50000 particles, all with the same fixed initial velocity $V_0 = 400\pi$. At $t = 0$, particles were located in a small region around $r = 0.7$, $\theta = 0$, and $\zeta = 0$, where $(r, \theta, \zeta)$ are toroidal coordinates. The evolution is initially very asymmetric because of the preferential direction induced by the drift in the motion of the particles along the eddies, which are aligned with the field lines. However, as particles go several times around the torus, $n(\theta, t)$ becomes increasingly symmetric. For this reason, we first remove the drift of the distribution of tracers and then we compare the evolution with the symmetric solution of the $\alpha = 1$ fractional diffusion equation on the circle (2). We show a few examples of this comparison in Fig. 3. The analytical solution seems to describe the numerical results relatively well.

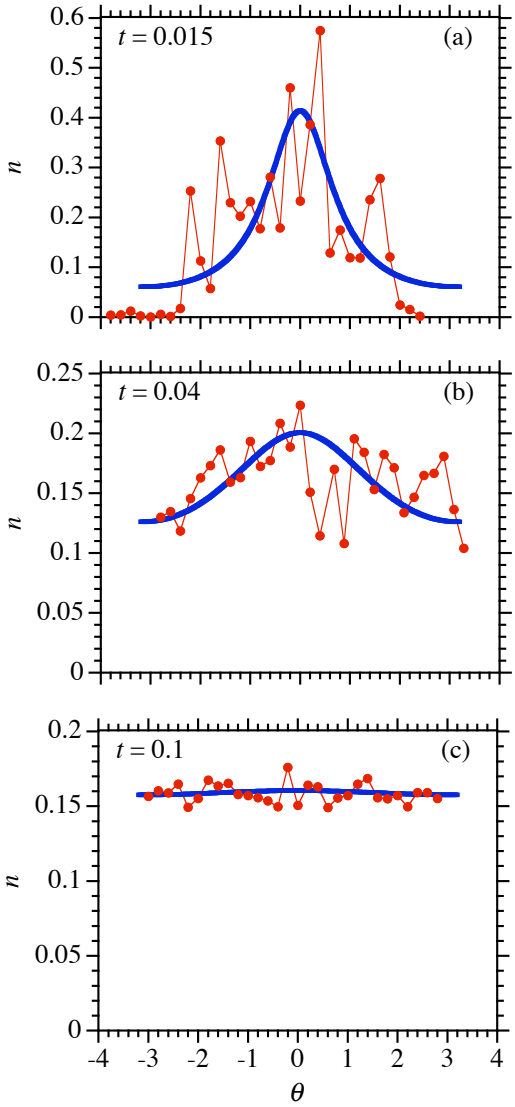


Figure 3: Comparison of the time evolution of the pdf of tracer particles with fixed initial toroidal velocity $V_0 = 400\pi$, and the analytical expression (2).

We have also calculated the time evolution of particle tracers with random initial velocities in the toroidal direction. We have used 50000 particles and the results of a typical calculation showing the evolution of $n(\theta, t)$ are plotted in Fig. 3, where one notes that the structures are gone. This is not surprising, but one of the expected consequences of the random velocity initialization of the tracers. What may be surprising is the change of the functional form of the distribution. These distributions do not look at all like the analytical distributions given by (2).

The explanation is simple. With a single initial velocity for all particles, at any given time they were all located at the same toroidal angle. Now, with the random initial velocities, at any given time the particles are distributed over a range of toroidal angles and what we have measured

is a poloidal distribution averaged over all the toroidal angles. Furthermore, since there is a mean drift associated with the twist of the magnetic field lines, in each toroidal plane $\zeta$, the poloidal distribution has its peak at a different value of $\theta$. In each toroidal plane $\zeta$, the analytical distribution is given by Eq. (2) with values a given value of $\zeta$ in the range $[-V_{\max}t, V_{\max}t]$. Here $V_{\max} = 400\pi$ is the maximum velocity of the tracers. Therefore, to reproduce the measured poloidal distribution, we have to average the fixed $\zeta$ distribution over the toroidal angle, that is

$$\langle n\rangle(\theta,t) = \frac{1-e^{-2\sigma t/\tau}}{2\pi}\frac{1}{2V_{\max}t}\int_{-V_{\max}t}^{V_{\max}t}\frac{d\zeta}{1-2e^{-\sigma t/\tau}\cos(\theta-u\zeta)+e^{-2\sigma t/\tau}}, \tag{3}$$

where $u$ is the average pitch of the field line at the radial position of the initial tracers. After some algebra, one obtains

$$\begin{aligned}\langle n\rangle(\theta,t) &= \frac{1}{2\pi u V_{\max}t}\left\{\arctan\left[\frac{1+e^{-\sigma t/\tau}}{1-e^{-\sigma t/\tau}}\tan\left(\frac{\theta+uV_{\max}t}{2}\right)\right]\right.\\ &- \left.\arctan\left[\frac{1+e^{-\sigma t/\tau}}{1-e^{-\sigma t/\tau}}\tan\left(\frac{\theta-uV_{\max}t}{2}\right)\right]\right\}.\end{aligned} \tag{4}$$

In Fig. 4 we show the excellent agreement between the analytical and numerical calculations for $\langle n\rangle$.

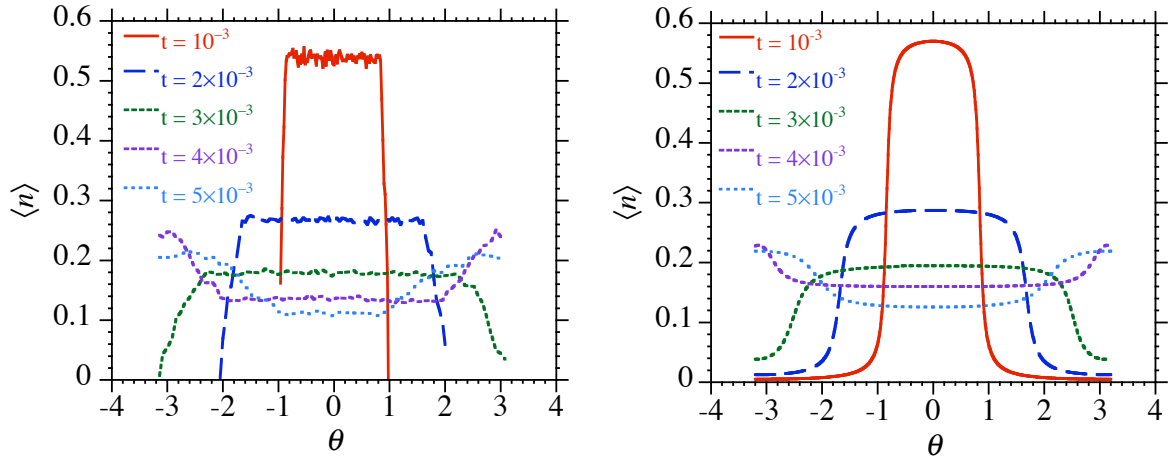


Figure 4: Numerical (left) and analytical (right) results for the averaged distribution of tracers

## References


[1] L. Garcia, B. A. Carreras, and V. E. Lynch, Phys. Plasmas **9**, 47 (2002).

[2] B. A. Carreras, V. E. Lynch, L. Garcia, et al., Chaos **13**, 1175 (2003).

[3] H. R. Strauss, Phys. Fluids **20**, 1354 (1977).

[4] J. F. Drake and T. M. Antosen, Jr., Phys. Fluids **27**, 898 (1984).

[5] I. Calvo, L. Garcia, B. A. Carreras, et al., Phys. Plasmas **15**, 042302 (2008).

[6] I. Calvo, B. A. Carreras, R. Sánchez, et al., J. Phys. A: Math. Theor. **40**, 13511 (2007).